STRESSES IN PLATES WITH A HOLE USING BOUNDARY ELEMENT METHOD

by

M. G. RAJASEKARAN

DEPARTMENT OF MECHANICAL ENGINEERING

INDIAN INSTITUTE OF TECHNOLOGY, KANPUR

JUNE, 1987

STRESSES IN PLATES WITH A HOLE USING BOUNDARY ELEMENT METHOD

A Thesis Submitted
In Partial Fulfilment of the Requirements
for the Degree of

MASTER OF TECHNOLOGY

by
M. G. RAJASEKARAN

to the

DEPARTMENT OF MECHANICAL ENGINEERING

INDIAN INSTITUTE OF TECHNOLOGY, KANPUR

JUNE, 1987

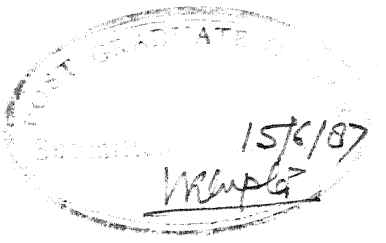

CERTIFICATE

This is to certify that the thesis entitled 'STRESSES IN PLATES WITH A HOLE USING BOUNDARY ELEMENT METHOD' by M.G. RAJASEKARAN, is a bonafide record of work done by him under our guidance and supervision, for the award of the degree of Master of Technology in the Indian Institute of Technology, Kanpur. The work carried out in this thesis has not been submitted elsewhere for the award of a degree.

Dr. V.SUNDARARAJAN
Professor,
Deptt. of Mech. Engg.,
IIT KANPUR

Dr. ASHWINI KUMAR
Professor,
Deptt. of Civil Engg.,
IIT KANPUR

(THESIS SUPERVISORS)

ACKNOWLEDGEMENTS

I, acknowledge with sincerity and gratitude, the guidance provided by Dr.V. Sundararajan and Dr. Ashwini Kumar, in sorting out various problems through the course of this thesis. I, also thank them for their contributions, made by way of timely advices and criticisms.

June 12, 1987
IIT KANPUR

M.G. Rajasekaran

CONTENTS

LIST OF FIGURES

LIST OF TABLES

NOMENCLATURE

Symbol	What the symbol represents
Savin[1]	Name of the author and the reference number
σ_{jk}	Stress tensor
u_k	Displacement component
p_k	Traction component
Γ	Boundary
Ω	Domain
-	The variable above the bar appears is prescribed as a boundary condition
R, R_1, R_2	Error terms on the domain and different parts of the boundary
*	Weighting field
eq. (2.1.1)	Equation number
ϵ_{jk}	Strain tensor
Δ	Dira Delta function
E	Young's Modulus
G	Rigidity Modulus
ν	Poisson's ratio
δ_{ij}	Kronecker Delta
n_j	Outward normal to the boundary at x
β	Source point
x	Field point
r	Distance between x and
r_i	Directional distance between x and
r^i	Derivative of r with respect to x_i
ci	Coefficient of ui when i is a point on the boundary
N	Number of boundary elements
l	Length of the element
g, h	Submatrices obtained after integrating u^*_{ij} & p^*_{ij}
G, H	Assembled matrix of g and h
U, P	Column vector of displacement and traction
I	'Unit' column vector
O	'Zero' column vector
σ_θ	Stress in the direction θ (hoop stress)
p	Applied stress

continued.....

Symbol	What the symbol represents
A, B, C	The three points at which stress concentration factors have been computed
d	Diameter of the circular cutout
a, b	Minor and major axis of the elliptical cutout
w	Width of the finite strip and finite plate
E_1, E_2	Young's modulus in longitudinal and transverse direction for composite materials
s_{11}, s_{12}} s_{22}, s_{66}}	Compliance matrix components for Composite materials

Consistent tensor notation has been used throughout. Subscripts i,j,k and l have been used as indices, the range being 1 to 2, unless otherwise indicated. Repetition of the index indicates the summation of the variable over the range of the index and a ',' represents differentiation with respect to that index of the variable.

ABSTRACT

Boundary element method has been used to compute the stress concentration factors for various plane stress problems, with circular and elliptical cutouts. The problems include an infinitely long strip, but finite in its width and a finite plate, both of them under uniform tensile streeses. The media selected are both isotropic and orthotropic in nature. Most of the problems have been done using both linear and constant elements. Wherever possible, results have been compared with experimental values and analytical solutions.

CHAPTER 1

INTRODUCTION AND LITERATURE SURVEY

1.1 Introduction

The boundary element method (**BEM**), appropriately called the boundary integral equation method (**BIEM**) is being increasingly used to solve solid mechanics problems especially when it concerns the stresses on the boundary or a crack tip, for example, stress concentration factor, fracture mechanics and contact problems. In this work, an effort has been made to study the stress concentration factors for various classical and other related problems using **BEM**.

For elastostatic problems, the method typically starts with weighted residual statement of the equilibrium equation. The weighting functions are chosen in such a way that the error distribution terms over the domain become zero and the "**domain terms disappear**"; only the boundary integrals will remain. With discretization of the boundary and substitution of proper boundary conditions, namely, displacements and tractions, this boundary integral equation can be solved to obtain the unknown values on the boundary, which can be later

utilised to compute the domain properties (stresses, displacements etc.)

1.2 Literature Survey

The problem of an infinite plate with a circular cutout has been solved analytically by **Kirsch**, which has beeen referred to by most of the literature in solid mechanics, including **Savin**[1]. On the same lines many problems have been solved and results have been presented by **Savin**[1]. The problems include a finite strip (infinite in its length and finite in its width) with symmetrically placed circular hole. **Heywood**[2] has done photoelastic analysis of the same problem and his results match with that presented by **Savin**[1].

Later on finite element method was used by **Chong and Pinter**[3] to solve the same problem; their results are slightly different from that predicted by **Heywood**[2], as d/w (d is the diameter of the circular hole and w is the width of the infinitely long strip) approaches 1. But for all the other values of d/w, their results compound the validity of the results presented by others[1,2].

Based on the guidelines provided by **Brebbia**[4,5,6], Boundary Element Method was used to solve the same problem; though, with constant element the results were not agreeing very well with others[1,2,3], linear element gave the results which were very close to that presented by them[1,2,3]. Using the program developed for constant element, various problems of finite strip with elliptical hole and finite plate with circular and elliptical hole were solved.

In the orthotropic case, **Lekhnitskii**[7] has solved a few problems of elliptical and circular hole in an infinite medium, as a plane stress problem. **Rizzo and Shippy**[8], later presented fundamental solutions for plane stress orthotropic problems and a procedure exactly same as that of isotropic boundary element was used by them to solve a few problems in this medium. Their results were agreeing very well with that presented by **Lekhnitskii**[7]. **Mahajerin and Sikarskie**[9] have used almost a similar scheme to predict the stress concentration factor in a double lap joint under tension.

The problems of elliptical hole in an infinite orthotropic medium were solved, based on the fundamental solution presented by **Rizzo and Shippy**[8], otherwise the

method is very similar to that used for isotropic medium. The results obtained were matching within 10% of those given in **Lekhnitskii**[7]. This program of constant element was used to get the data regading the stress concentration factors for finite strip and finite plate with circular and elliptical cutout.

Results have been presented for finite and infinite plate with circular and elliptical hole for both isotropic and orthotropic media. Most of the cases were studied with both linear and constant boundary elements. Wherever possible results have been compared with analytical and experimental results.

CHAPTER 2

BEM FORMULATION

2.1 Weighted Residual Statement

Statement of the problem in elastostatics without body force is as follows[4]:

$$\sigma_{jk,j} = 0 \quad \text{with boundary conditions}$$
$$u_k = \bar{u}_k \quad \text{on} \quad \Gamma_1$$
$$p_k = \bar{p}_k \quad \text{on} \quad \Gamma_2 \qquad (2.1.1)$$

where σ_{jk} is the stress tensor
u_k is the displacement component
p_k is the traction component
$\bar{}$ means the variable is prescribed as a boundary condition
Γ is the boundary enclosing the domain Ω

Tensor notation has been used throughout; repetition of an index denotes summation over the range of that index and a ',' indicates partial differentiation with respect to the $\mathbf{variable}_{\mathbf{index}}$ (here, for example $\mathbf{x}_j$). The numbers within the square brackets indicate the reference number.

The generalised weighted residual statement used in finite elements and other techniques is [4]

$$\int_{\Omega} R\, w\, d\Omega = \int_{\Gamma_2} R_2\, w\, d\Gamma - \int_{\Gamma_1} R_1\, (\partial w/\partial n)\, d\Gamma \qquad (2.1.2)$$

The same weighted residual statement written for the elastostatics problem defined by eq. (2.1.1) will be[5]

$$\int_{\Omega} \sigma_{jk,j} u^*_k d\Omega = \int_{\Gamma_2} (p_k - \bar{p}_k) u^*_k d\Gamma - \int_{\Gamma_1} (u_k - \bar{u}_k) p^*_k d\Gamma \qquad (2.1.3)$$

where '*' indicates the weighting field.

2.2 Formulation

Integrating eq. (2.1.3) once

$$\int_{\Omega} \sigma_{jk} \epsilon^*_{jk} d\Omega = -\int_{\Gamma_2} \bar{p}_k u^*_k d\Gamma - \int_{\Gamma_1} p_k u^*_k d\Gamma + \int_{\Gamma_1} (\bar{u}_k - u_k) p^*_k d\Gamma$$

where ϵ_{jk} indicates the strain tensor.

Noting that[4] $\sigma_{jk}\epsilon^*_{jk} = \sigma^*_{jk}\epsilon_{jk}$, we have

$$\int_{\Omega} \sigma^*_{jk} \epsilon_{jk} d\Omega = -\int_{\Gamma_2} \bar{p}_k u^*_k d\Gamma - \int_{\Gamma_1} p_k u^*_k d\Gamma + \int_{\Gamma_1} (\bar{u}_k - u_k) p^*_k d\Gamma \qquad (2.2.1)$$

Integrating once again

$$\int_{\Omega} \sigma^*_{jk,j} u_k d\Omega = -\int_{\Gamma_2} \bar{p}_k u^*_k d\Gamma - \int_{\Gamma_1} p_k u^*_k d\Gamma + \int_{\Gamma_1} \bar{u}_k p^*_k d\Gamma + \int_{\Gamma_2} u_k p^*_k d\Gamma$$

The above equation without boundary condition can be written as

$$\int_{\Omega} \sigma^*_{jk,j} u_k d\Omega = \int_{\Gamma} u_k p^*_k d\Gamma - \int_{\Gamma} p_k u^*_k d\Gamma \qquad (2.2.2)$$

Now we try to eliminate the domain integral by satisfying the equilibrium equation in the following manner[6]

$$\sigma^{*}_{jk,j} + \Delta^{i}_{l} = 0 \qquad (2.2.3)$$

where Δ^{i}_{l} is the **Dirac Delta** function and hence represents a unit force at a point **i** in direction **l**. A traction and displacement field denoted as $\mathbf{p^{*}_{lk}}$ and $\mathbf{u^{*}_{lk}}$ can be obtained from this equation; these will be the fundamental solutions to be used in **eq. (2.2.2)**. Substituting **eq. (2.2.3)** into **eq. (2.2.2)**, we obtain

$$u^{i}_{l} + \int_{\Gamma} u_{k} p^{*}_{lk} d\Gamma = \int_{\Gamma} p_{k} u^{*}_{lk} d\Gamma \qquad (2.2.4)$$

where u^{*}_{lk} and p^{*}_{lk} are fundamental displacement and traction in direction **k** due to unit force in direction **l**.

2.3 Fundamental Solution

Equation (2.2.2) has been solved analytically and the fundamental solutions have been presented in many of the text-books[4,5,6]. The fundamental solution to be used in the present formulation are that of two-dimensional isotropic

plane strain problem, which are as follows:

$$u^*_{ij} = \frac{1}{8\pi G(1-\nu)}\left[(3-4\nu)\ln\left(\frac{1}{r}\right)\delta_{ij} + r_{,i}r_{,j}\right]$$

$$p^*_{ij} = \frac{-1}{4\pi(1-\nu)r}\left[\frac{-\partial r}{\partial n}\{(1-2\nu)\delta_{ij} + 2r_{,i}r_{,j}\} - (1-2\nu)(r_{,i}n_j - r_{,j}n_i)\right] \qquad (2.3.1)$$

Here, the point at which the unit force is applied is called the **source point** (denoted as β) and the point at which we compute the numerical value of the fundamental solution is called the **field point** (denoted as x). The field point is always located on the boundary, whereas the source point may be inside the domain or on the boundary.

In the above fundamental solution and elsewhere

G is the rigidity modulus
ν is the Poisson's ratio
r is the distance between the source point and the field point
n_j is the outward normal to the boundary at the field point
δ_{ij} is the Kronecker delta

All the derivatives are taken with respect to the field point x.

To obtain fundamental solution for the plane stress case, the substitution of ν by $\nu/(1+\nu)$ will suffice.

2.4 Boundary Integral Equation

In eq. (2.2.4) the point i is inside the domain. We can take it to the boundary as a limiting case and this results in a slightly different equation of the form[5]

$$c_i u_l^i + \int_\Gamma u_k p_{lk}^* d\Gamma = \int_\Gamma p_k u_{lk}^* d\Gamma \qquad (2.4.1)$$

This is the boundary integral equation (BIE) and can be solved numerically to obtain the unknown boundary values (u on Γ_1 and p on Γ_2). Once all the boundary values are known, eq. (2.2.4) can be used to obtain displacement(s) in the domain. Alternately, we may wish to obtain stresses in the domain directly by using

$$\sigma_{ij} = \frac{2G}{1-2\nu}\delta_{ij}\frac{\partial u_l}{\partial x_l} + G\left[\frac{\partial u_i}{\partial x_j} + \frac{\partial u_j}{\partial x_i}\right] \qquad (2.4.2)$$

where $(\partial u_i/\partial x_j)$ can be obtained from eq. (2.2.4). After making the substitution for $(\partial u_i/\partial x_j)$ eq. (2.4.2) becomes

$$\sigma_{ij} = \int_\Gamma D_{kij} p_k d\Gamma - \int_\Gamma S_{kij} u_k d\Gamma \qquad (2.4.3)$$

where

$$D_{kij} = \frac{1}{4\pi(1-\nu)r}\left[(1-2\nu)\{\delta_{ki}r_{,j}+\delta_{kj}r_{,i}-\delta_{ij}r_{,k}\}+2r_{,i}r_{,j}r_{,\underline{k}}\right]$$

$$S_{kij} = \frac{G}{2\pi(1-\nu)r}\left[2\frac{\partial r}{\partial n}\{(1-2\nu)\delta_{ij}r_{,k}+\nu(\delta_{ik}r_{,j}+\delta_{jk}r_{,i})\right.$$
$$-4r_{,i}r_{,j}r_{,k}\}+2\nu(n_i r_{,j}r_{,k}+n_j r_{,i}r_{,k})$$
$$+(1-2\nu)(2n_k r_{,i}r_{,j}+n_j\delta_{ik}+n_i\delta_{jk})$$
$$\left.-(1-4\nu)(n_k\delta_{ij})\right] \qquad (2.4.4)$$

CHAPTER 3

NUMERICAL IMPLEMENTATION

3.1 Procedure

Writing eq. (2.4.1) for any point on the boundary, we have:

$$c_{ij}u_j + \int_{\Gamma} p^*_{ij}u_j d\Gamma = \int_{\Gamma} u^*_{ij}p_j d\Gamma \qquad (3.1.1)$$

The main steps involved in numerical implementation can be written down as:

(i) Discretization of the boundary Γ into N elements over which the displacements and the tractions may be assumed to be piecewise interpolated. This way eq. (3.1.1) gives 2 linear algebraic equations with 4N vairables.

(ii) Similar equations for all i=1,N will be 2N in number, which means it will give us a system of linear algebraic equations with 2N unknowns. For each node the number of degrees of freedom is 4, namely, u_1, u_2, p_1 and p_2, out of

which 2 will be specified as **boundary conditions** and the rest of the 2 unknowns per node will make it to **2N** unknowns.

(iii) Use any standard method to solve this system of equations and obtain the other boundary values.

(iv) The same procedure is adopted while computing the stresses or displacements in the domain, except that these values will be obtained directly after computing their respective boundary integrals.

3.2 Types of Element

The boundary elements, for two-dimensional problems, as the name indicates, will be line elements on the boundary. Usually the degrees of freedom will be traction (**p**) and displacement (**u**) in **x** and **y** directions, numbering to 4. Depending upon the distribution of these properties over the element, the elements can be classified as constant, linear, quadratic and so on.

For constant element, the distribution of **u** and **p** will be uniform or constant and the representative point will be the geometrical mid-point of the element itself. For linear

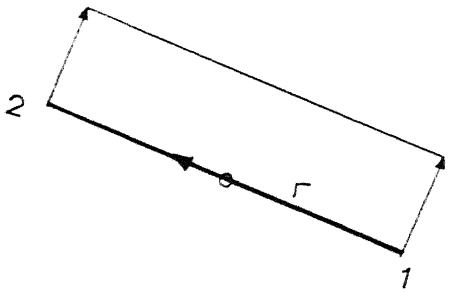

Constant

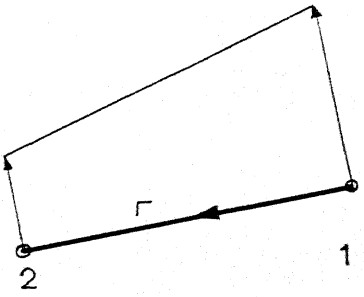

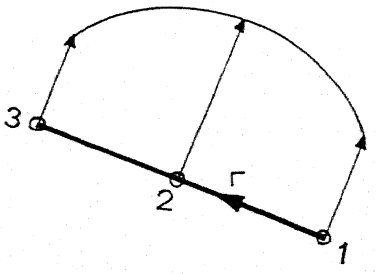

Quadratic

Linear

FIG. 3.2.1 Different types of element

element, a linear distribution is assumed between the two extreme ends of the element and for quadratic element a parabolic variation may be assumed with another point in the middle of the element (refer fig. 3.2.1).

In this work, most of the computations have been done using constant element and, unless otherwise indicated, all the numerical implementations have been done for the constant element.

3.3 Discretization and Computation of Eq. (3.1.1)

Equation (3.1.1) in a discretized form can be rewritten as follows:

$$c_{ij}u_j + \sum_{j=1}^{N}\left[\int_{\Gamma_j} p^*_{ij}u_j\,d\Gamma\right] = \sum_{j=1}^{N}\left[\int_{\Gamma_j} u^*_{ij}p_j\,d\Gamma\right] \qquad (3.3.1)$$

Integration over each element j is done by using **Gaussian Quadrature**. The number of points taken for this is usually 4; in some cases variable number of points have been used. The (directional) distances (r_i) and other derivatives are given by the following expressions (see fig. 3.3.1)

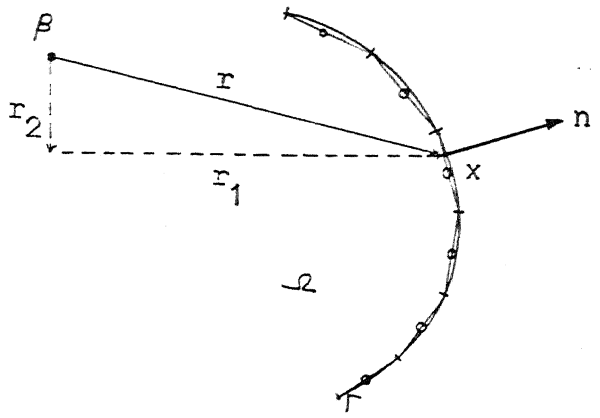

FIG. 3.3.1 Integration on the boundary

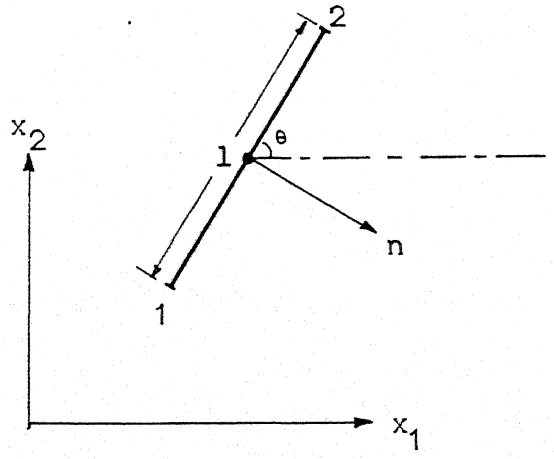

FIG. 3.3.2
Analytical evaluation of g_{ii}

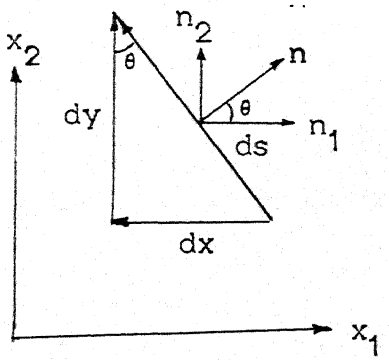

FIG. 3.7.1
ds/dx_i

$$r_i = x_i(x) - x_i(\beta)$$
$$r = (r_i r_i)^{1/2}$$
$$r_{,i} = (\partial r/\partial x_i(x)) = r_i/r$$
$$(\partial r/\partial n) = r_{,i} n_i \qquad (3.3.2)$$

As we see the numerical computation of u^*_{ij} and p^*_{ij} over **j** with respect to **i** does not pose any problem when **i≠j**. The values obtained after numerically computing the integral of u^*_{ij} and p^*_{ij} are called as **g** and **h** submatrices, each of which is **2x2**. But when **i=j**, u^*_{ij} has **ln(1/r) singularity** which can be evaluated analytically[5] (refer fig.3.3.2), the results of which have been reproduced below:

$$g_{11} = \frac{1}{8\pi G(1-\nu)} \left[(3-4\nu)\left(1-\ln\frac{l}{2}\right) + \left(\frac{r_1}{l}\right)^2 \right]$$

$$g_{12} = g_{21} = \frac{r_1 r_2}{8\pi G(1-\nu) l}$$

$$g_{22} = \frac{1}{8\pi G(1-\nu)} \left[(3-4\nu)\left(1-\ln\frac{l}{2}\right) + \left(\frac{r_2}{l}\right)^2 \right] \qquad (3.3.3)$$

where l is the length of the element.

Hence diagonal **g** submatrices can be evaluated analytically. Even though the diagonal **h** submatrices have not been computed we will start assembling them in accordance with eq. (3.3.1).

3.4 Assembly of the Discretized Equation (3.3.1)

For any point **i** on the boundary, eq. (3.3.1), after discretization and assembly will take the following form:

$$c_{ii}u_i + \begin{bmatrix} h_{i1} & h_{i2} & \cdots & h_{ij} & \cdots & h_{iN} \end{bmatrix} \begin{Bmatrix} u_1 \\ u_2 \\ \vdots \\ u_j \\ \vdots \\ u_N \end{Bmatrix} =$$

$$\begin{bmatrix} g_{i1} & g_{i2} & \cdots & g_{ij} & \cdots & g_{iN} \end{bmatrix} \begin{Bmatrix} p_1 \\ p_2 \\ \vdots \\ p_j \\ \vdots \\ p_N \end{Bmatrix}$$

Varying **i** from **1** to **N** we have the following system of equations, represented in the matrix form.

$$\begin{bmatrix} h_{11} & h_{12} & \cdots & h_{1j} & \cdots & h_{1N} \\ h_{21} & h_{22} & \cdots & h_{2j} & \cdots & h_{2N} \\ \vdots & \vdots & \cdots & \vdots & \cdots & \vdots \\ h_{i1} & h_{i2} & \cdots & h_{ij} & \cdots & h_{iN} \\ \vdots & \vdots & \cdots & \vdots & \cdots & \vdots \\ h_{N1} & h_{N2} & \cdots & h_{Nj} & \cdots & h_{NN} \end{bmatrix} \begin{Bmatrix} u_1 \\ u_2 \\ \vdots \\ u_j \\ \vdots \\ u_N \end{Bmatrix} =$$

$$\begin{bmatrix} g_{11} & g_{12} & \cdots & g_{1j} & \cdots & g_{1N} \\ g_{21} & g_{22} & \cdots & g_{2j} & \cdots & g_{2N} \\ \vdots & \vdots & \cdots & \vdots & \cdots & \vdots \\ g_{i1} & g_{i2} & \cdots & g_{ij} & \cdots & g_{iN} \\ \vdots & \vdots & \cdots & \vdots & \cdots & \vdots \\ g_{N1} & g_{N2} & \cdots & g_{Nj} & \cdots & g_{NN} \end{bmatrix} \begin{Bmatrix} p_1 \\ p_2 \\ \vdots \\ p_j \\ \vdots \\ p_N \end{Bmatrix} \qquad (3.4.1)$$

where $h_{ii} = \underline{h}_{ii} + c_{ii}$

We have evaluated neither $\underline{h}_{ii}$ nor c_{ii}. In matrix notation eq. (3.4.1) can be rewritten as

$$[H]\ \{U\} = [G]\ \{P\} \qquad (3.4.2)$$

But now h_{ii} can be directly obtained from the consideration of rigid-body movements[4] in a bounded or unbounded body. If we have a unit displacement in any one direction eq. (3.4.2) then becomes

$$[H]\ \{I_1\} = \{O\}$$

in which I_1 is a vector defining unit rigid displacement in direction 1. Therefore the diagonal submatrices are simply

$$h_{ii} = - \sum_{i \neq j} h_{ij} \qquad (3.4.3)$$

Thus there was no necessity to find out c_{ii} and h_{ii} explicitly. But the same condition for an unbounded body (infinite or semi-infinite) becomes[4]

$$h_{ii} = I - \sum_{i \neq j} h_{ij} \qquad (3.4.4)$$

3.5 Solving the system

Now eq. (3.4.2) is complete in the sense that we know H and G matrix completely, and we can directly substitute the boundary conditions in the form of displacements and/or tractions, at each node. The total number of unknowns after this will be 2N and eq. (3.4.2) can be rearranged as:

$$[A] \{X\} = \{B\} \qquad (3.5.1)$$

where A contains the rearranged coefficients, B is the column-vector (obtained by multiplying the proper coefficients with the known boundary conditions) and X is the unknown column-vector. X in eq. (3.5.1) can be obtained using standard procedures available for solving system of linear algebraic equations.

To keep track of the known/unknown tractions and displacements, a system of coding has been used. For example, KODE=1 means traction specified and KODE=0 means displacement prescribed at that node, in **x** or **y** direction. This coding system will be able to sort out the **X** vector (now containing the solution) properly into traction and displacement vectors.

3.6 Domain Displacements and Stresses

Once we know the displacements and tractions over the entire boundary, then, for displacement we can use **eq.** (2.2.4) and for stress **eq.** (2.4.4) can be used. The discretization to be adopted will be the same as that used for **eq.** (3.3.1) and exactly the same procedure will be employed for this. But now the only difference will be that, there will be no singular integrals, because the point under consideration is inside the domain.

3.7 Surface Stresses

Evaluation of stresses on the boundary may also be done taking the load point to the boundary, as a limiting case of

equation eq. (2.4.4). But this will lead to very inaccurate results, mainly because the tensor components involve singular integrals. Hence another scheme presented by **Rizzo and Shippy**[8] can be very easily implemented without having to undergo the cumbersome procedure of evaluating singular integrals. The scheme is outlined below:

We have seven unknowns on the boundary, namely 3 stress components (σ_{ij}) and 4 displacement gradient components ($u_{i,j}$). Also we have

$$p_j = \sigma_{ij} n_i \tag{3.7.1}$$

along with stress-strain relationships (3 in number). This amounts to 5 equations. We need two more equations. They can be got by evaluating du_i/ds (along the boundary) numerically and equating it to analytical expression for the same.

$$\begin{aligned} \frac{du_i}{ds} &= \frac{du_i}{dx_1}\frac{dx_1}{ds} + \frac{du_i}{dx_2}\frac{dx_2}{ds} \\ &= u_{i,1}(dx_1/ds) + u_{i,2}(dx_2/ds) \end{aligned} \tag{3.7.2}$$

From fig. 3.7.1

$$\begin{aligned} (dx_1/ds) &= -\sin\theta = -n_2 \\ (dx_2/ds) &= \cos\theta = n_1 \end{aligned} \tag{3.7.3}$$

Substituting this into eq. (3.7.2)

$$(du_i/ds) = u_{i,2}n_1 - u_{i,1}n_2 \qquad (3.7.4)$$

where s has been used to indicate the boundary.

Now we have a system of 7x7 linear algebraic equations, which can be solved to give the stresses on the surface or the boundary.

4.8 Composition of h_{ii}

As we have seen already h_{ii} can be computed by considering the rigid-body movements, either in a bounded or unbounded medium. But for constant elements, for which the boundary is smooth[4], an analytical evaluation of h_{ii} can be done. By letting the point i go to the boundry, the first boundary integral in eq. (2.4.1) can be evaluated as[5]

$$\begin{bmatrix} -0.5 & 0 \\ 0 & -0.5 \end{bmatrix}$$

Hence h_{ii} submatrix will be

$$\begin{bmatrix} 1 & 0 \\ 0 & 1 \end{bmatrix} + \begin{bmatrix} -0.5 & 0 \\ 0 & -0.5 \end{bmatrix} = \begin{bmatrix} 0.5 & 0 \\ 0 & 0.5 \end{bmatrix} \qquad (3.8.1)$$

CHAPTER 4

RESULTS AND DISCUSSION

4.1 Program

A simple program with constant boundary element was developed to start with, to handle two dimensional elastostatic problems in isotropic media with **single continuous boundary**. Then additional features like surface stresses, variable Gauss points for integration (depending upon the distance from the boundary element and its length) were introduced. The program was also extended to handle **two boundary** problems. In fact, it can easily be extended to take into consideration any number of boundaries. Using this program stress concentration factors were obtained for finite and infinite plate with circular and elliptical holes at its centre. The same problems were repeated with **linear element program** available in [4].

Then a constant element program was developed for orthotropic media, with almost the same features as for the corresponding isotropic case. The major changes required were: fundamental solutions u^*_{ij} and p^*_{ij} and their derivatives. These have been discussed in detail in succeeding sections. This program was used to compute the

stress concentration factors in orthotropic media for similar problems. Before this a check was made to test the authenticity of the program by comparing the results of the classical problems presented by **Lekhnitskii**[7]. In all the cases σ_θ/p has been computed where **p** is the applied stress.

4.1 Isotropic Problems

The classical problem of infinite plate with a hole was solved; the resulting stress concentration factor was 3.001 as against 3 obtained analytically by **Kirsch**. For the case with elliptical hole, a result of 4.962 was obtained, the analytical result being 5. In these problems, where constant element was used, half of the plate was considered for analysis instead of the usual one quarter. The reason for doing this was that the constant element's representative point is the mid-point of the element and at points where we have corners, we cannot expect to compute the stresses accurately (eg., the point of maximum stress in the problems under consideration, that is point **B** in fig.4.2.1); however small the element is chosen at this point, the stresses computed will not be at point **B**, but slightly away from it and hence it is bound to be inaccurate. A half plate can

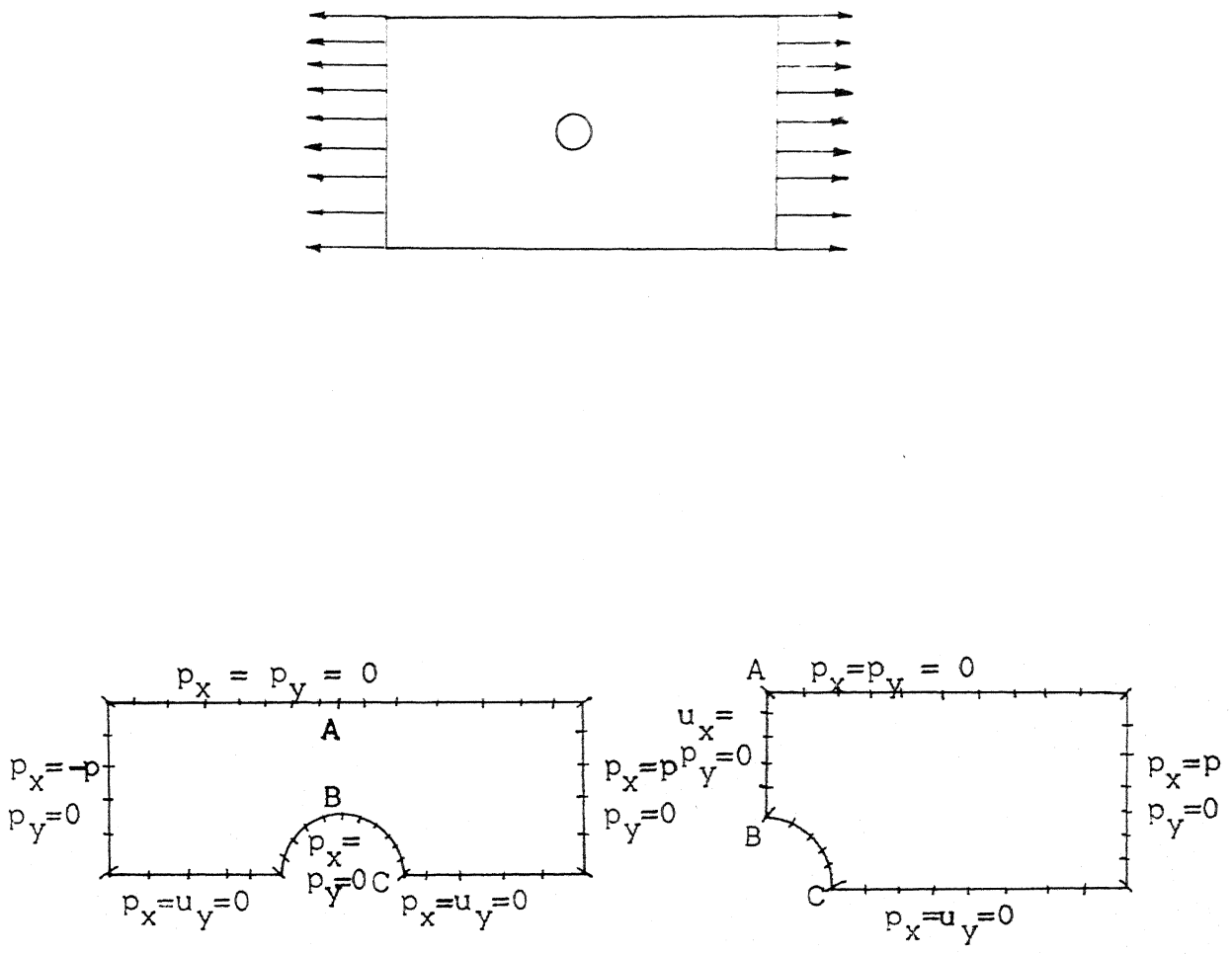

FIG 4.2.1 Different models adopted

consider such a point B by having a constant element symmetrical about y axis and in this case the mid-point of the element itself happens to be B.

For a d/w ratio of 0.1, the number of elements used were 54, 19 of them on the semi-circle, The problem was repeated for various d/w ratio from 0.2 to 0.9, for a finite strip and also for a finite plate with circular and elliptical hole. As this ratio is increased, the hole, either circular or elliptical also increases in size. Hence, a different and very fine mesh size on the boundary was used each time. ~~Through~~ The mesh size has not been reported for each of the case; the validity of the same was checked by observing the composition of h_{ii} submatrix, which has to be $\begin{bmatrix} 0.5 & 0 \\ 0 & 0.5 \end{bmatrix}$ in the case of constant element, as already indicated

All the problems were solved using Linear Element Program given in [1]. Because of the nature of the linear element, the advantage was taken of the bi-axial symmetry, and only a quarter of the plate was considered for analysis.

The results of finite strip with (i) circular hole and (ii) elliptical hole under uniform tension at infinity have been presented in Table 4.1 and 4.2, respectively. The

results of finite plate under uniform tension with (i) circular hole and (ii) elliptical hole have been presented in Table 4.3 and 4.4, respectively.

For the case of finite strip under uniform tension at inifinity, with circular hole, the **FEM** solution by **Chong and Pinter**[3], the experimental results by **Heywood**[2] and the analytical solution by **Savin**[1] have been presented for ready reference.

For the maximum stress concentration factor at B, it can be seen that the constant element results match with other results for lower ratios of **d/w** and deviate very much as **d/w** approaches 0.9. On the other hand, the linear element results almost match even at a higher ratio of 0.8. For the point **C**, where the stress is compressive, the results obtained by constant element are very much less than those by linear element and are not accurate. This is to be expected since the constant element is represented by a point which will be just above **C**. The linear element, however, gives a more accurate result, since the nodes are at the extreme ends for this type of element. (refer fig. 4.2.2)

FIG.4.2.2 Advantages of linear element

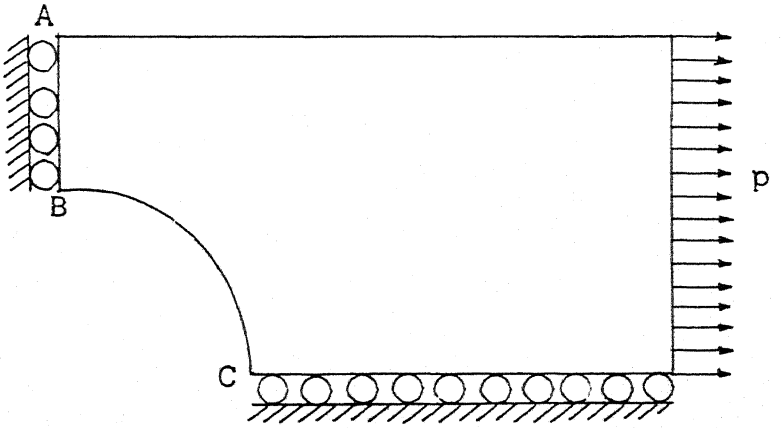

FIG.4.2.3 Quarter-plate model

Stresses obtained for the point A first decrease from 1 to somewhere near 0.75 and then increases upto 4 as **d/w** ratio increases. Before discussing this, let us have a look at the modelling done for this case (refer fig.4.2.3). The model almost looks similar to that of a beam loaded in the longitudinal direction, with a notch included at its base. The boundary conditions of this model are, of course, slightly different from that of a beam. From this figure, we can say that apart from a tensile stress, there will also be a moment which will alter the state of stress at **A** and **B**. For the point **B** the bending moment will yield more tensile stresses, whereas for the point **A** it will be compressive. Because of this, the overall stress at **A** tends to reduce upto a certain value of **d/w**. Beyond this **d/w** ratio, the plate does not behave anymore like this and its short area at the base, entirely takes up the applied load; with the result the stress distribution is non-linear across the base, with both the points **A** and **B** under larger tensile stresses.

But from Tables 4.3 and 4.4, which show the results for finite plate with circular and elliptical hole, the behaviour is very much as we expected. The stresses at **A** decreases from almost **p** to near 0 for **d/w** = 0.4, and then becomes negative (or compressive). In the case of finite plate, it

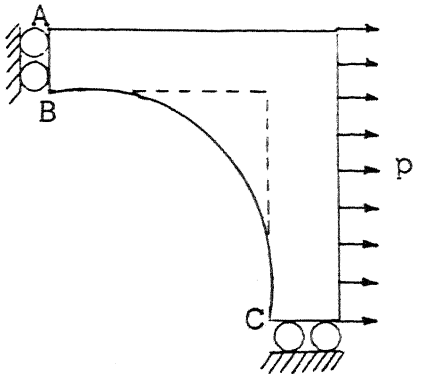

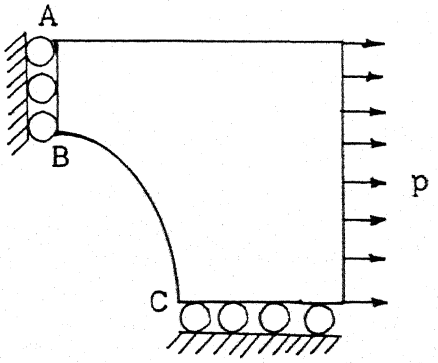

FIG. 4.2.4 Models for finite plate

is obvious that the model looks like a L-beam for circular hole (refer fig.4.2.4). This clearly shows why the stress at A goes on decreasing as d/w ratio increases from 0.1 to 0.9. But for the case with elliptical hole, once again the effect is not that much as that with a circular hole. This may be because the ellipse approximates to a notch at the base; but the plate is not long enough to behave like a beam. Hence the state of stress at A for this case is somewhere between that of the previous two cases (Tables 4.2 and 4.3).

4.3 Orthotropic Case

The major changes required for the orthotropic case were (i) the fundamental solution, (ii) the stress-strain relationship and (iii) the derivatives of the fundamental solution which were later used in computing the displacement and stresses in the domain.

The fundamental solution in the case of orthotropic case is more complicated than that of isotropic case and involves a lot of material dependent constants to be evaluated. The plane stress fundamental solution given by **Rizzo and Shippy**[8] has been reproduced here:

$$u^*_{11} = K_a[\sqrt{\alpha_1}A_2^2 \ln r_1 - \sqrt{\alpha_2}A_1^2 \ln r_2]$$

$$u^*_{12} = u^*_{21} = -K_a A_1 A_2(\theta_1 - \theta_2)$$

$$u^*_{22} = -K_a[A_1^2 \ln r_1/\sqrt{\alpha_1} - A_2^2 \ln r_2/\sqrt{\alpha_2}] \qquad (4.3.1)$$

$$p^*_{11} = K_a[A_1/(\sqrt{\alpha_2}\, r_2^2) - A_2/(\sqrt{\alpha_1}\, r_1^2)]x_k n_k$$

$$p^*_{12} = K_a[M_1 A_2/r_1^2 - M_2 A_1/r_2^2]$$

$$p^*_{21} = K_a[M_1 A_1/(\alpha_1 r_1^2) - M_2 A_2/(\alpha_2 r_2^2)]$$

$$p^*_{22} = K_a[A_1/(\sqrt{\alpha_1}\, r_1^2) - A_2/(\sqrt{\alpha_2}\, r_2^2)]x_k n_k \qquad (4.3.2)$$

where

$$1/K_a = 2(\alpha_1 - \alpha_2)s_{22}$$

$$\alpha_1 + \alpha_2 = (2s_{12} + s_{66})/s_{22}$$

$$\alpha_1 \alpha_2 = s_{11}/s_{22}$$

$$A_i = s_{12} - \alpha_i s_{22}$$

$$r_i^2 = x_1^2 + (x_2^2/\alpha_i)$$

$$\theta_i = \arctan[x_2/(x_1\sqrt{\alpha_i})]$$

$$M_i = x_1 n_2 \sqrt{\alpha_i} - x_2 n_1/\sqrt{\alpha_i} \qquad (4.3.3)$$

The derivatives of the fundamental solutions in x and y directions are presented in Appendix A. This along with the plane stress constitutive equation was used for solving problems in orthotropic media. For all the orthotropic problems, the material properties chosen were that of birch plywood referenced in **Lekhnitskii**[7]. They are as follows:

$$s_{11} = 8.333 \times 10^{-6} \quad \text{sq-cm/kgf}$$
$$s_{12} = -0.6 \times 10^{-6} \quad \text{sq-cm/kgf}$$
$$s_{22} = 16.667 \times 10^{-6} \quad \text{sq-cm/kgf}$$
$$s_{66} = 143 \times 10^{-6} \quad \text{sq-cm/kgf}$$

First the problem of an infinite plate with an elliptical hole was considered for which analytical solutions are available in **Lekhnitskii**[7]. The results of both analytical and **BEM** solution are given in Table 4.5.

All the problems were done considering them as **two-boundary** problems, because of which the number of elements increased. 36 elements were used on the ellipse inside and 44 elements on the outer boundary, which was 100 times away from the ellipse as was the size of the ellipse. By **St. Venant's Principle**, the effect of the elliptical hole was not considered while imposing the boundary conditions on the symmetrical elements of the outer boundary (see fig. 4.3.1).

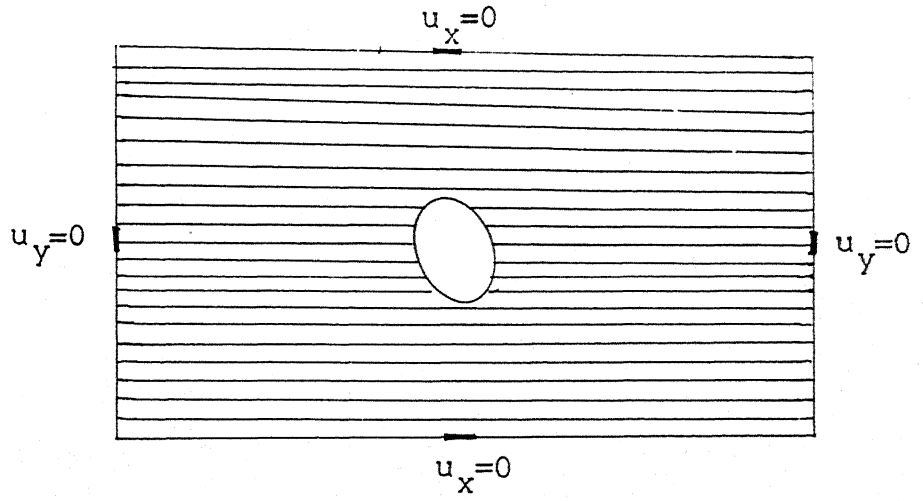

FIG. 4.3.1 Orthotropic plate with elliptical hole

On the elliptical hole $p_x = 0$ and $p_y = 0$ were the boundary conditions.

Table 4.5 clearly shows the accuracy of **boundary element method** for these type of problems in orthotropic media as well. Then a series of problems involving finite strip and finite plate with circular and elliptical holes were solved using the constant element program, the results of which have been presented in Tables 4.6 thru 4.11

Table 4.6 gives the stress concentration factors of a finite strip with circular hole, at points A, B and C (see the figure above the table) using constant boundary element and the medium being mildly orthotropic (for Birch-plywood $E_1/E_2 = 2$). The direction of loading is along the Longitudinal axis of the fibres. The pattern in which the stresses at the three mentioned points vary with the size of the hole is very similar to that of the isotropic case shown in table 4.1; only the values of the stress concentration factors are slightly higher than the corresponding values for the isotropic medium.

For the case of finite strip with elliptical hole, once again the same kind of similarity is exhibited as that of

isotropic case. For example in isotropic case the stress concentration factor at B is more for elliptical hole than that of circular hole. The same pattern is seen in orthotropic case also

For finite plate with circular and elliptical hole (Tables 4.7 and 4.8) another set of data was generated with transverse fibres. As has been reported by **Lekhnitskii**[7] the stress concentration factor (for maximum value of stress) for transverse fibres is less than that for longitudinal fibres. This feature is seen in both tables 4.7 and 4.8. Another behaviour to be noted is that at A stresses become compressive for both longitudinal and transverse fibres, like that of isotropic medium.

Another set of data was obtained for galss-epoxy composite material and this has been presented in tables 4.9 to 4.11. The properties of this composite material are [9]

$$s_{11} = 7.1053 \times 10^{-7} \text{ sq-cm/kgf}$$
$$s_{12} = -1.4921 \times 10^{-7} \text{ sq-cm/kgf}$$
$$s_{22} = 67.6423 \times 10^{-7} \text{ sq-cm/kgf}$$
$$s_{66} = 167.6848 \times 10^{-7} \text{ sq-cm/kgf}$$

The results in tables 4.9 to 4.11 for the case of glass-epoxy can be compared with those in tables 4.6 to 4.8 for birch-plywood. It is easily seen that the maximum stress concentration factor (at B) is always greater for glass-epoxy, whereas the minimum stress concentration (at C) is always less. This is the case with longitudinal fibres only; the situation is just the reverse for transverse fibres. This pattern in the stress concentration may be attributed to the strong orthotropic nature of glass-epoxy, for which E_1/E_2 is 9 as compared with birch-plywood, for which the same ratio is 2.

The stress pattern at A, however, is different from that at B and C. In the case of glass-epoxy, the stress at A is never compressive, with transverse fibres, while the situation was just the opposite for birch-plywood.

4.4 Conclusion

We can draw the following conclusions based on the results that have been obtained using the boundary element method:

1. Constant boundary elements give reasonably good results for a wide range of ratios of d/r and b/w in all the cases. But when this ratio is between 0.7 and 0.5, constant elements are not capable of modelling the stress concentration factor problems.

2. On the other hand linear elements give a very good result (see table 4.1) even for a ratio of 0.5. This is to be expected because, the variation of the properties over the elements are linear and hence more accurate than constant element.

3. For more accurate results, higher order elements with much more finer meshes should be used, with no approximation of the geometrical boundaries.

4. On the whole, boundary element method is much better method than many other approximate techniques, when it comes to the solving of stress concentration factor problems.

TABLE 4.1

E = 2 000 000 kgf/sq-cm ν = 0.1

Point B

σ_θ/p

d/w	(BEM) Const.	Linear	Savin	Heywood	FEM
0.1	3.001	3.05	3.03	3.032	-----
0.2	3.039	3.218	3.14	3.14	-----
0.3	3.239	3.435	3.36	3.347	3.449
0.4	3.562	3.797	3.74	3.693	3.83
0.5	4.07	4.379	4.32	4.25	4.413
0.7	6.017	6.847	----	6.747	7.166
0.8	8.086	9.524	----	10.002	10.276
0.9	12.81	15.734	----	20.01	19.544

d/w	A		C (-)	
	Const.	Linear	Const.	Linear
0.1	0.977	0.98	0.658	0.999
0.2	0.957	0.949	0.621	1.148
0.3	0.909	0.891	0.707	1.282
0.4	0.891	0.823	0.928	1.451
0.5	0.892	0.758	1.203	1.644
0.7	1.24	0.755	1.463	2.078
0.8	2.25	1.056	1.725	2.224
0.9	6.467	4.033	1.959	2.474

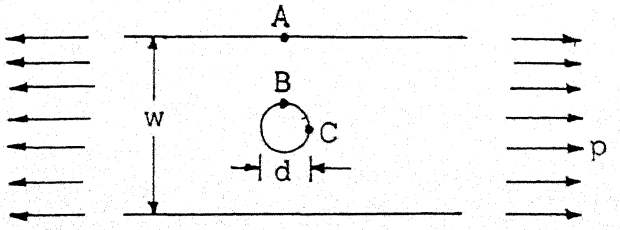

TABLE 4.2

E = 2 000 000 kgf/sq-cm b/a = 2 ν = 0.1

b/w	σ_θ/p A Const.	A Linear	B Const.	B Linear	C (-) Const.	C (-) Linear
0.1	0.985	0.99	4.962	4.935	0.523	1.
0.2	0.977	0.978	4.913	5.029	0.571	1.042
0.3	0.945	0.949	5.152	5.263	0.620	1.117
0.4	0.935	0.905	5.537	5.642	0.764	1.223
0.5	0.926	0.844	6.143	6.245	0.941	1.358
0.7	1.008	0.71	3.448	8.836	1.207	1.716
0.8	2.061	0.836	11.082	11.921	1.636	1.937
0.9	6.059	2.845	17.02	19.38	2.202	2.36

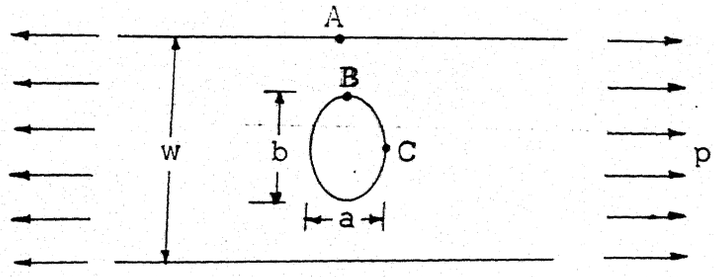

TABLE 4.3

E = 21 000 000 kgf/sq-cm ν = 0.3

σ_θ / p

d/w	A		B		C (-)	
	Const.	Linear	Const.	Linear	Const.	Linear
0.1	0.938	0.965	2.88	3.071	0.472	1.057
0.2	0.838	0.846	3.106	3.34	0.725	1.272
0.3	0.643	0.601	3.533	3.841	1.081	1.69
0.4	0.303	0.133	4.222	4.705	1.618	2.44
0.5	-0.252	-0.765	5.313	6.212	2.44	3.789
0.6	-1.076	-2.58	7.015	9.01	3.649	6.36
0.7	-2.005	-6.622	9.513	14.734	5.163	11.7
0.8	-1.833	-16.62	12.616	27.882	7.061	23.88
0.9	4.091	-35.54	16.48	54.	7.23	+43.8

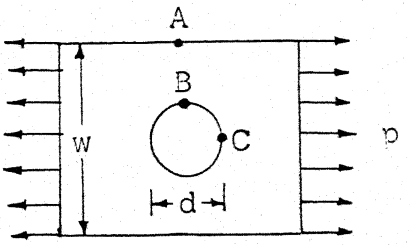

TABLE 4.4

E = 21 000 000 kgf/sq-cm b/a = 2 ν = 0.3

σ_θ/p

b/w	A		B		C (-)	
	Const.	Linear	Const.	Linear	Const.	Linear
0.1	0.952	0.978	4.68	0.481	1.036	1.036
0.2	0.891	0.905	4.988	5.268	0.703	1.156
0.3	0.777	0.765	5.461	5.785	0.934	1.377
0.4	0.589	0.525	6.15	6.556	1.238	1.737
0.5	0.303	0.131	7.097	7.66	1.654	2.3
0.6	-0.098	-0.49	8.436	9.257	2.22	3.125
0.7	-0.571	-1.423	10.428	11.672	2.966	4.632
0.8	-0.798	-2.65	13.795	15.685	3.895	6.18
0.9	1.442	-2.98	21.517	24.13	4.928	8.77

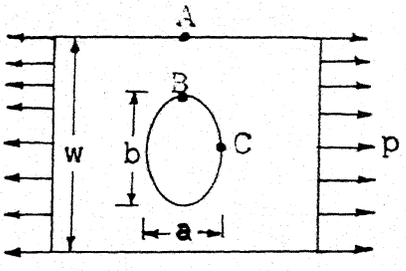

TABLE 4.5

BIRCH PLYWOOD b/a = 2 CONSTANT ELEMENT

σ_θ / p

Major Axis inclination to fibres (degrees)	MAXIMUM BEM	MAXIMUM LEKH.	MINIMUM (-) BEM	MINIMUM (-) LEKH.
	LONGITUDINAL FIBRES			
90	10.62	9.91	0.669	0.71
60	7.14	8.2	0.669	1.11
45	6.099	5.84	0.696	0.46
30	5.062	4.92	0.677	0.77
0	3.24	3.23	0.615	0.71
	TRANSVERSE FIBRES			
180	7.56	7.2	1.33	1.41
150	5.6	6.14	1.25	1.53
135	4.67	4.98	1.39	1.57
120	3.82	3.8	1.28	1.54
90	2.56	2.57	1.13	1.41

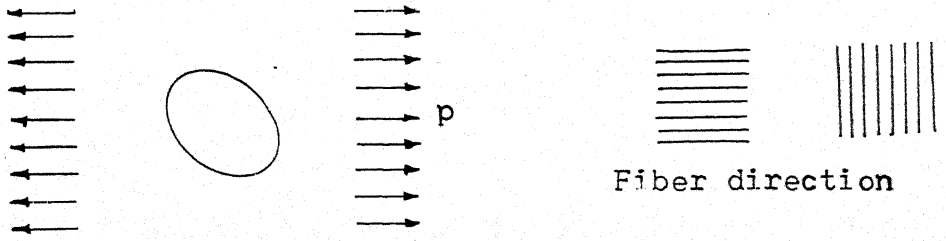

TABLE 4.6

BIRCH PLYWOOD — CONSTANT ELEMENT

σ_θ / p

d/w or b/w	A	B	C (-)
	CIRCULAR HOLE		
0.1	0.996	5.677	0.671
0.2	0.971	5.809	0.745
0.3	0.942	6.055	0.849
0.4	0.925	6.452	0.976
0.5	0.937	7.07	1.122
0.6	1.002	8.044	1.287
0.7	1.187	9.664	1.468
0.8	1.778	12.684	1.654
0.9	4.877	19.99	1.863
	ELLIPTICAL HOLE (b/a = 2)		
0.1	1.003	10.71	0.673
0.2	0.997	10.898	0.71
0.3	0.988	11.247	0.77
0.4	0.983	11.804	0.854
0.5	0.991	12.666	0.96
0.6	1.034	14.021	1.093
0.7	1.184	16.273	1.26
0.8	1.682	20.493	1.466
0.9	4.312	30.826	1.708

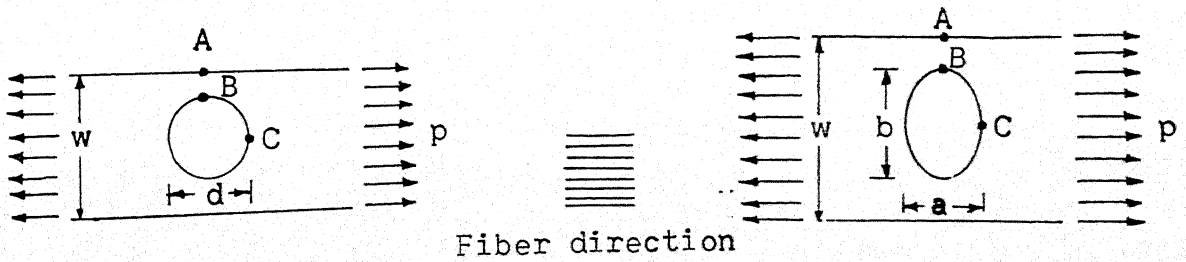

TABLE 4.7

BIRCH PLYWOOD — CONSTANT ELEMENT

σ_θ / p

d/w	A L	A T	B L	B T	C (-) L	C (-) T
0.1	0.963	0.968	5.922	4.33	0.736	1.443
0.2	0.833	0.871	6.659	4.706	0.989	1.873
0.3	0.563	0.692	1.716	5.305	1.468	2.653
0.4	0.082	0.412	9.22	6.169	2.254	3.942
0.5	-0.737	-0.2	11.366	7.429	3.494	5.988
0.6	-2.13	-0.69	14.72	9.336	5.44	9.308
0.7	-4.386	-1.633	19.864	12.26	8.394	14.495
0.8	-7.134	-2.208	27.29	16.427	12.253	21.771
0.9	-5.347	1.744	36.876	22.633	15.706	28.609

L - Longitudinal Fibres (with usual properties[6])

T - Transverse Fibres (with s_{11} and s_{22} interchanged)

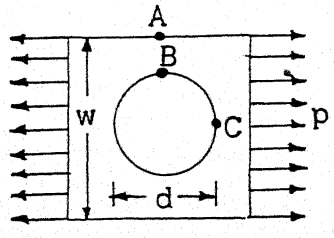

Fiber direction

TABLE 4.8

BIRCH PLYWOOD b/a = 2 CONSTANT ELEMENT

σ_θ / p

b/w	A L	A T	B L	B T	C (-) L	C (-) T
0.1	0.974	0.98	11.11	7.762	0.719	1.412
0.2	0.887	0.92	12.3	8.293	0.88	1.648
0.3	0.704	0.806	13.9	9.078	1.165	2.065
0.4	0.379	0.628	15.893	10.094	1.594	2.684
0.5	-0.136	0.385	18.32	11.376	2.196	3.538
0.6	-0.879	0.102	21.457	13.045	3,018	4.679
0.7	-1.809	-0.132	25.492	15.395	4.113	6.159
0.8	-2.59	-0.024	31.307	19.379	5.504	7.982
0.9	-1.353	1.985	43.339	29.714	7.11	10.169

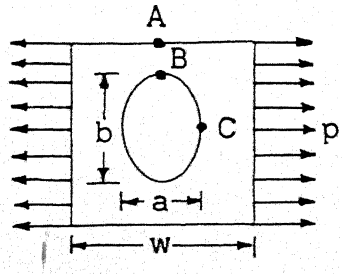

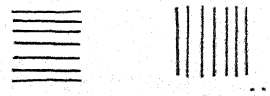

Fiber direction

TABLE 4.9

GLASS EPOXY — CONSTANT ELEMENT

σ_θ/p

d/w or b/w	A	B	C (-)
	CIRCULAR HOLE		
0.1	0.974	7.146	0.339
0.2	0.923	7.23	0.361
0.3	0.912	7.32	0.38
0.4	0.899	7.617	0.407
0.5	0.884	8.227	0.45
0.6	0.889	9.275	0.506
0.7	0.962	11.137	0.566
0.8	1.306	14.62	0.643
0.9	3.671	23.183	0.723
	ELLIPTICAL HOLE (b/a = 2)		
0.1	0.982	13.666	0.333
0.2	0.954	13.774	0.345
0.3	0.964	13.885	0.354
0.4	0.971	14.314	0.372
0.5	0.971	15.211	0.403
0.6	0.978	16.736	0.449
0.7	1.035	19.426	0.505
0.8	1.330	24.289	0.58
0.9	3.379	36.598	0.759

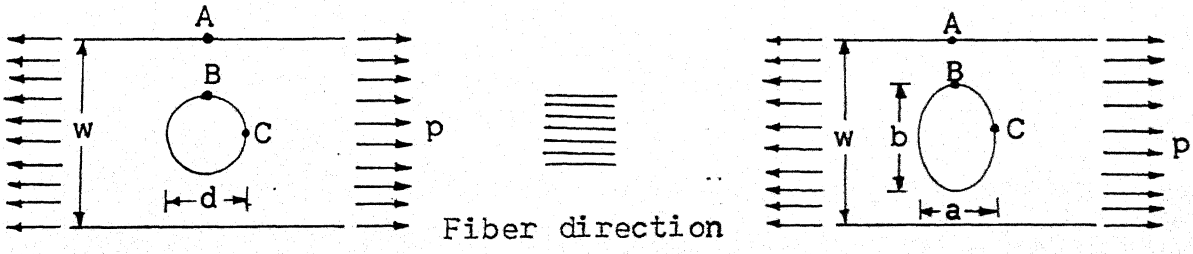

TABLE 4.10

GLASS-EPOXY CONSTANT ELEMENT

σ_e/p

d/w	A L	A T	B L	B T	C (-) L	C (-) T
0.1	0.962	0.982	7.18	2.78	0.342	3.031
0.2	0.818	0.939	8.328	2.935	0.465	3.728
0.3	0.489	0.887	9.882	3.212	0.695	4.855
0.4	-0.16	0.831	12.103	3.638	1.062	6.562
0.5	-1.332	0.794	15.121	4.269	1.617	9.077
0.6	-3.37	0.815	19.89	5.198	2.423	13.183
0.7	-6.714	1.078	26.878	6.559	3.507	19.438
0.8	-11.202	2.348	37.217	8.56	4.631	28.476
0.9	-11.744	7.785	50.902	12.811	5.298	36.136

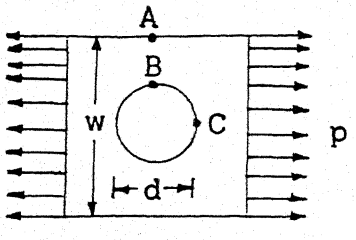

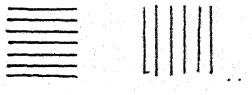

Fiber direction

TABLE 4.11

GLASS-EPOXY b/a = 2 CONSTANT ELEMENT

σ_θ/p

b/w	A L	A T	B L	B T	C (-) L	C (-) T
0.1	0.974	0.991	13.726	4.53	0.336	3.034
0.2	0.864	0.971	15.696	4.698	0.425	3.38
0.3	0.62	0.938	18.234	4.99	0.579	3.94
0.4	0.145	0.901	21.559	5.433	0.805	4.703
0.5	-0.696	0.877	25.592	6.084	1.118	5.69
0.6	-2.086	0.907	31.191	7.067	1.545	6.976
0.7	-4.19	1.09	38.484	8.668	2.125	8.623
0.8	-6.748	1.751	48.529	11.733	2.87	10.586
0.9	-6.968	4.596	63.195	20.238	3.686	13.217

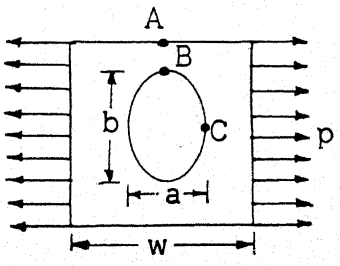

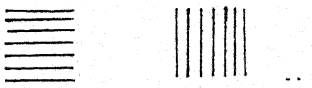

Fiber direction

REFERENCES

[1] SAVIN G.N., Stress concentration factor around holes, Permagon Press (1961)

[2] HEYWOOD R.B., Designing by Photoelasticity, Chapman & Hall Ltd., (1952)

[3] CHONG K.P. and PINTER W.J., Stress concentrations of tensile strips with large holes, Computers and Structures, v19,n4,p583-589 (1984)

[4] BREBBIA C.A., TELLES J.C.F. and WROBEL L.C., Boundary Element Techniques - Theory and Application in Engineering, Springer-Verlag (1984)

[5] BREBBIA C.A., The Boundary Element Method for Engineers, Pentech Press (1978)

[6] BREBBIA C.A. and WALKER S., Boundary Element Techniques in Engineering, Newnes-Butterworths (198Ø)

[7] LEKHNITSKII S.G., Theory of Elasticity of an Anisotropic Body, Mir Publishers (1981)

[8] RIZZO F.J. and SHIPPY D.J., A method for stress determination in plane anisotropic bodies, J. of Composite Materials, v4,p36-61 (197Ø)

[9] MAHAJERIN E. and SIKARSKIE D.L., Boundary Element Study of a Loaded Hole in an Orthotropic plate, J. of Composite Materials, v2Ø,p375-389 (1986)

APPENDIX - A

The derivatives of the fundamental solution in the case of plane stress orthotropic problems is given below. These are used in computing the stresses in the domain.

$$u_{11,1} = K_a x_1 [(\sqrt{\alpha_2} A_1^2/r_2^2) - (\sqrt{\alpha_1} A_2^2/r_1^2)]$$

$$u_{11,2} = K_a x_2 [A_1^2/(r_2^2\sqrt{\alpha_2}) - A_2^2/(r_1^2\sqrt{\alpha_1})]$$

$$u_{12,1} = u_{21,1} = K_a A_1 A_2 x_2 [1/(\sqrt{\alpha_2} r_2^2) - 1/(\sqrt{\alpha_1} r_1^2)]$$

$$u_{12,2} = u_{21,2} = K_a A_1 A_2 x_1 [1/(\sqrt{\alpha_2} r_2^2) - 1/(\sqrt{\alpha_1} r_1^2)]$$

$$u_{22,1} = K_a x_1 [A_1^2/(r_1^2\sqrt{\alpha_1}) - A_2^2/(r_2^2\sqrt{\alpha_2})]$$

$$u_{22,2} = K_a x_2 [A_1^2/(r_1^2\alpha_1^{3/2}) - A_2^2/(r_2^2\alpha_2^{3/2})]$$

$$p_{11,1} = K_a [2x_1 x_k n_k \{A_1/(\sqrt{\alpha_2} r_2^4) - A_2/(\sqrt{\alpha_1} r_1^4)\} - n_1 \{A_1/(\sqrt{\alpha_2} r_2^2) - A_2/(\sqrt{\alpha_1} r_1^2)\}]$$

$$p_{11,2} = K_a [2x_2 x_k n_k \{A_1/(\alpha_2^{3/2} r_2^4) - A_2/(\alpha_1^{3/2} r_1^4)\} - n_2 \{A_1/(\sqrt{\alpha_2} r_2^2) - A_2/(\sqrt{\alpha_1} r_1^2)\}]$$

$$p_{12,1} = K_a [A_2 \{2x_1 M_1/r_1^4 - \sqrt{\alpha_1} n_2/r_1^2\} - A_1 \{2x_1 M_2/r_2^4 - \sqrt{\alpha_2} n_2/r_2^2\}]$$

$$P_{12,2} = K_a[A_2\{2x_2M_1/(\alpha_1 r_1^4) + n_1/(\sqrt{\alpha_1}\, r_1^2)\}$$

$$- A_1\{2x_2M_2/(\alpha_2 r_2^4) + n_1/(\sqrt{\alpha_1}\, r_2^2)\}]$$

$$P_{21,1} = K_a[A_1\{2x_1M_1/r_1^4 - \quad n_2/r_1^2\}/$$

$$- A_2\{2x_1M_2/r_2^4 - \quad n_2/r_2^2\}/ \quad]$$

$$P_{21,2} = K_a[A_1\{2x_2M_1/(\sqrt{\alpha_1}\, r_1^4) + n_1/(\quad r_1^2)\}/\alpha_1$$

$$- A_2\{2x_2M_2/(\alpha_2 r_2^4) + n_1/(\sqrt{\alpha_2}\, r_2^2)\}/\alpha_2]$$

$$P_{22,1} = K_a[2x_1x_kn_k\{A_1/(\sqrt{\alpha_1}\, r_1^4) - A_2/(\sqrt{\alpha_2}\, r_2^4)\}$$

$$- n_1\{A_1/(\sqrt{\alpha_1}\, r_1^2) - A_2/(\sqrt{\alpha_2}\, r_2^2)\}]$$

$$P_{22,2} = K_a[2x_2x_kn_k\{A_1/(\alpha_1^{3/2} r_1^4) - A_2/(\alpha_2^{3/2} r_2^4)\}$$

$$- n_2\{A_1/(\sqrt{\alpha_1}\, r_1^2) - A_2/(\sqrt{\alpha_2}\, r_2^2)\}]$$

where the usual notations have been used and all the constants have been explained in the fundamental solution itself.